# Slippery sounds

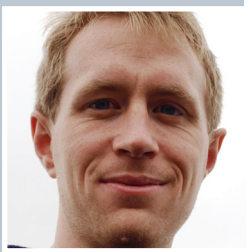

Michael Gedge

Paul Stoodley

Martyn Hill

*Gedge, Stoodley and Hill describe a new method for protecting marine sensors from biofouling.*

### Who should read this paper?

Biologists with an interest in the response of microorganisms to acoustic stimulus; specialists in the use of ultrasound for various applications; and, of course, anyone with an interest in marine biofouling and how to mitigate it will all have an interest in reading this paper.

### Why is it important?

Objects in a marine environment can quickly become coated with a surface layer of biofilm. Biofilms are formed when bacteria adhere to wetted surfaces and excrete a slime-like substance which then aids the adherence of other microorganisms such as fungi, yeast and algae. It has been shown that these biofilms can have disruptive effects on ocean sensors within one week of deployment in seawater. For optical sensors, the physical presence of biofilm lowers the sensitivity and efficiency of the sensor. For chemical based sensors, the metabolic activity of the organisms that make up the biofilm can create strong chemical gradients, which will affect the readings. This is problematic for in-situ ocean sensors since regular cleaning by hand is not practical. Automated mechanical and chemical cleaning options exist, but are expensive and can reduce the working life of the sensor. Ultrasound is widely used in laboratories and elsewhere to clean instruments. However, this method relies on high energy acoustic streaming which requires power of some 35-45 Watts. In this paper, the authors present a novel low power (<1 W) ultrasonic technique to reduce the formation of biofilm on the surface of ocean sensors. The work is currently at an early technology readiness level and further development is required before the technology could be commercially exploited.

### About the authors

Michael Gedge received his B.Eng. from the University of Southampton in 2008 and has since been working toward a PhD degree at the same institution. He specializes in ultrasonic standing wave technology, in particular with a view to incorporating the technology into oceanographic sensors. Paul Stoodley is a Professor in the Departments of Microbial Infection and Immunity and Orthopedics at the Ohio State University, and a Visiting Professor of Microbial Tribology with the National Centre for Advanced Tribology at Southampton University. His research interests focus on how bacteria attach, grow, and persist as biofilms on medical, dental, industrial, and marine surfaces. Martyn Hill is Head of Engineering Sciences and Professor of Electromechanical Systems at the University of Southampton. His research is largely focused on the manipulation of cells and particles in microfluidic systems, particularly through the use of ultrasonic radiation forces.

# MINIMIZING BIOFOULING IN MICROFLUIDIC DEVICES THROUGH THE USE OF CONTINUOUS ULTRASONIC STANDING WAVES

**Michael Gedge[1], Paul Stoodley[1,2], Martyn Hill[1]**
*[1]Engineering Sciences, University of Southampton, United Kingdom*
*[2]Center for Microbial Interface Biology, Ohio State University, Columbus, OH, United States*

## ABSTRACT

This paper describes a novel low power method to reduce biofilm formation in microfluidic channels. When an ultrasonic (≈2 MHz) standing wave is set up across a microfluidic channel (≈ 250 μm) the resulting pressure amplitude can move small particles to the pressure node or anti-node, depending on the properties of the particle. This effect has been applied to *Vibrio natriegens* within poly(methyl methacrylate) (PMMA) microfluidic channels and a reduction in biofilm formation has been seen over a period of a week. This is a novel low power biofilm reduction strategy.

## INTRODUCTION

The Earth's oceans host an enormous range of natural resources, over 90 billion kg of fish and shell fish are caught each year [WOR, 2010]. The oceans play an overriding role in climate regulation, removing vast quantities of carbon from the atmosphere. It is believed phytoplankton could account for more than half the Earth's oxygen production [Field et al., 1998]. Monitoring these biological and chemical characteristics offers an invaluable insight into the way our oceans work, which can then be used to generate and verify reliable models of the global ecosystem. Existing methods for carrying out such monitoring are expensive, coarse in terms of spatial and temporal sampling, and involve risk of sample contamination and degradation. Remote in-situ microfluidic sensors are being developed to fulfil this need for data; these sensors must be small, robust, reliable, and power-efficient.

Sensors left in a marine environment suffer from the effects of biofilm accumulation. Biofilms are comprised of microorganisms and extracellular polymeric substance (EPS) and start to form when bacteria adhere to a wetted surface. The bacteria then excrete a slime-like EPS which aids the adherence of other microorganisms such as fungi, yeast, algae, and other bacteria species [Salta et al., 2013]. It has been shown that these films can have disruptive effects on sensors within a week [Lehaitre et al., 2008]. When microorganisms come into contact with a surface, they attach themselves in a matter of seconds to minutes. As the biofilm grows and matures, cells and small clumps continually detach into the overlying fluid from mechanical shear or through a co-ordinated dispersal process [Hall-Stoodley et al., 2004]. The presence of biofilms will have detrimental effects on the performance of marine sensors. In optical

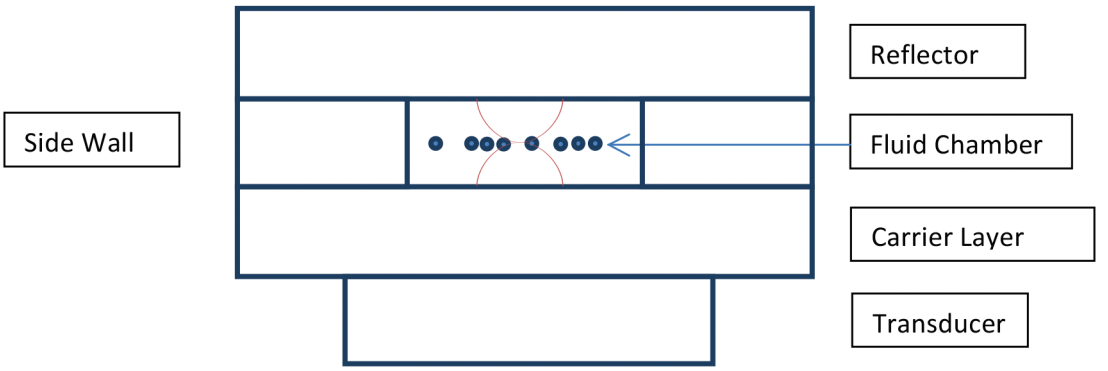


Figure 1: A diagram of a typical planar resonator device with a half wave resonant mode in the fluid chamber. Particles will be moved to form a plane parallel to the transducer. The red lines indicate the pressure amplitude within the acoustic standing wave.

based sensors, the presence of biofilms in the optical path will affect readings, lowering sensitivity and efficiency. For chemical based sensors, the metabolic activity of the organisms within the biofilm can create strong chemical gradients (i.e., pH and dissolved oxygen) which will affect the readings [Delauney et al., 2010]. These factors are especially problematic for in-situ sensors as regular cleaning by hand is not possible. Mechanical and chemical cleaning options exist but are either expensive or will reduce the working life of the system because of high power requirements. The formation of biofilms in microfluidic channels will also have detrimental effects on flow rates and could eventually lead to microchanneling in the device and eventually clogging. For these reasons it is important to protect in-situ oceanographic sensors from biofouling.

Previously, ultrasonic techniques have been shown to remove biofilms from surfaces [Sankaranarayanan et al., 2008; Bott, 2000]. While effective, these methods rely on high energy acoustic streaming which places significant power requirements on the sensor [Delauney et al., 2010; Whelan and Regan, 2006]. Some experiments report power consumption in the region of 35-45 W for effective biofilm removal [Mott et al., 1998]. In this paper, we present a novel low power (<1 W) ultrasonic technique to reduce the formation of biofilms within marine micro sensors.

## FORCES ON PARTICLES WITHIN AN ULTRASONIC STANDING WAVE

Particles such as cells experience forces when in an acoustic field [Bruus, 2012A; Wang and Lee, 1998]. These acoustic radiation forces cause particles to move to the pressure node or anti-node of a wave. Acoustic radiation forces have been known since the late 19th century [Kundt and Lehman, 1874] and have found an increasing range of applications recently. Standing waves create much larger forces on small particles than travelling waves, as the amplitudes of the two counter propagating waves superimpose to generate significant energy gradients (Figure 1).

Analytical solutions to the forces acting on a particle in an acoustic field are well documented

[King, 1934; Gor'Kov, 1962]. The following solution by Yosioka and Kawasima is frequently used and it predicts the radiation force acting on a small compressible sphere within a planar field [Yosioka and Kawasima, 1955].

$$F = 4\pi k r^3 \epsilon \phi(\rho, \beta) \sin(2kx) \qquad (1)$$

where $\epsilon$ denotes the energy density, $\phi$ the acoustic contrast factor, and $k$ the wave number in the fluid, given by $k=2\pi/\lambda$. The acoustic contrast factor controls the direction of the force on the particle. A positive acoustic contrast factor results in particles moving to the pressure node. A negative acoustic contrast factor will move particles to the pressure anti-node. The acoustic contrast factor is defined by the following equation:

$$\phi(\rho, \beta) = \frac{\rho_f + \frac{2}{3}(\rho_p - \rho_f)}{2\rho_p + \rho_f} - \frac{\beta_p}{3\beta_f} \qquad (2)$$

where $\rho$ denotes density and $\beta$ compressibility, with subscripts $_p$ and $_f$ denoting the particle or the fluid, respectively. Hard dense objects such as glass will have a high positive acoustic contrast factor. Compressible buoyant particles such as lipids will have a high negative acoustic contrast factor. Generally speaking, cells have a positive acoustic contrast factor thus will be forced to the pressure nodes.

Acoustic energy gradients within a standing wave will also generate forces on the fluid medium itself, causing flows known as acoustic streaming [Sadhal, 2012; Lei et al., 2014]. The viscous drag forces that such flows impart on particles become increasingly significant relative to the acoustic radiation forces as the particle size is reduced.

## ULTRASONIC FORCES ON MARINE BACTERIA

To counteract the problems associated with biofouling, it was proposed to use ultrasonic standing waves to limit the growth of biofilms within microfluidic devices. Ultrasonic standing wave technology should be well suited to the reduction of biofilm formation: bacteria tend to have positive acoustic contrast factors, meaning cells will move to the pressure nodes, coupled with the fact that pressure nodes tend to be positioned away from the walls of fluid channels [Augustsson et al., 2009; Townsend et al., 2004]. Although there are many species of bacteria with a large variation in cell size which ranges between 0.3 μm and 750 μm [Chien et al., 2012], in general, most bacteria tend to be of the order 0.5-2 μm in size [Srivastava and Srivastava, 2003]. For these particle sizes and with excitation frequencies in the low MHz range, drag forces due to streaming and acoustic radiation forces are of a similar magnitude [Bruus, 2012B]. Recent work has shown that sub-micron sized bacteria can be successfully manipulated with acoustophoresis [Antfolk et al., 2014; Carugo et al., 2014] and in the application considered here, ordered focusing of the bacteria is not required so the radiation forces and the streaming-induced movement are both likely to reduce the likelihood of bacteria-wall interactions reducing the chance of them adhering and replicating, although it should be noted that the ultrasonic forces generated are not expected to reduce the viability of the bacteria [Hultstrom et al., 2007; Wiklund, 2012].

As a starting point, *Vibrio natriegens* were chosen as the test bacterial species. *V.*

*natriegens* are a marine species that form biofilms and also have a rapid growth rate (sub 10 minute replication time in optimal conditions at 37° Centigrade) and are considered non-pathogenic [Eagon, 1962]. *Vibrio natriegens* have a measured volume of 0.93 ± 0.06 $\mu m^3$ in a dormant state and 3.5 ± 0.5 $\mu m^3$ in a growing state [Fagerbakke et al., 1996]. The lower bound of the dormant state is comparable to a 0.59 µm radius sphere. Cells are typically rod shaped with dimensions 0.606 µm wide x 0.5 µm thick x 3.334 µm long, measured using atomic force microscopy [Cheng et al., 2010]. A solution of minimal marine media with nutrients (3MN) was selected as the fluid as it is commonly used for cultivating bacteria [Denkin and Nelson, 1999; Mårdén et al., 1985]. The aim of this work was to apply and optimize ultrasonic standing waves to significantly reduce the formation of biofilm growth in microfluidic channels.

The following parameters were used to calculate the acoustic contrast factor of bacteria cells. Cell compressibility has been assumed to be similar to red blood cells as there is very little data available regarding the compressibility of bacteria. Red blood cells are considered relatively compressible (i.e., closer to the compressibility of water), so using this value is conservative and is expected to underestimate the acoustic contrast factor and therefore the forces generated.

Cell density: 1.031-1.212 g $cm^{-3}$, typical for bacteria in water [Sharma et al., 1998].
Cell compressibility: 3.38 x $10^{-10}$ $m^2$ $N^{-1}$ [Toubal et al., 1999].
3MN solution density: 1.0235 g $cm^{-3}$.
Speed of sound in 3MN: 1508 m $s^{-1}$ [Coates, 1990].

The compressibility of the fluid can be calculated using the following formula.

$$\beta_f = \frac{1}{\rho_f c_f^2} \quad (3)$$

The calculated compressibility of the 3MN solution is 4.3 x $10^{-10}$ $m^2$ $N^{-1}$; this is close to the value of 4.5 x $10^{-10}$ $m^2$ $N^{-1}$ for pure water [Fitts, 2013]. From here it is possible to estimate the acoustic contrast factor of bacteria cells using Equation 2. The calculated acoustic contrast factor of a bacteria cell is between 0.074 and 0.126, confirming a net resultant force towards the pressure node. This is comparable to the acoustic contrast factor of polystyrene beads in pure water of 0.15, which are used frequently in ultrasonic standing wave devices due to their cell-like properties.

## POLYMER DEVICES

The majority of ultrasonic standing wave devices tend to be made from materials such as glass and silicon. For this technology to be applicable to marine micro sensors, it was adapted for use in polymers. There is much interest in polymer ultrasonic particle devices despite the associated higher losses. This is because they can be produced cheaply, allowing them to be used as disposable devices. Polymers are also often transparent, making them ideal for imaging.

PMMA films supplied by Cadillac Plastic were identified as a suitable material for the production of polymer ultrasonic devices. Films were available in the following

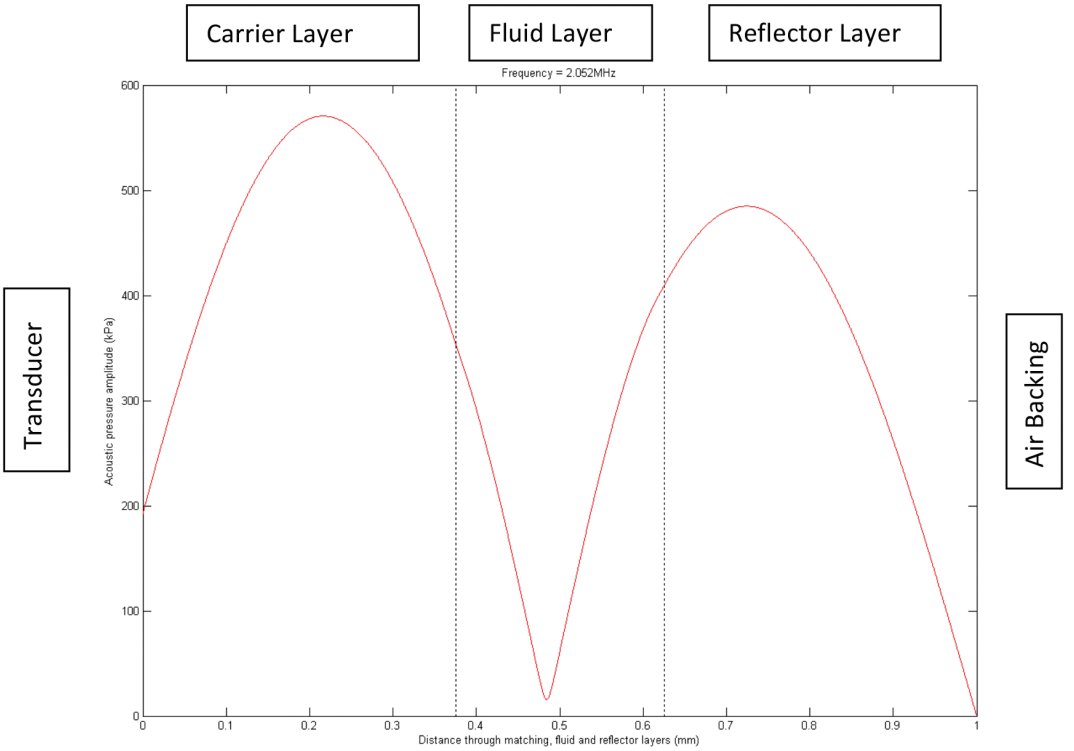


Figure 2: An example pressure plot of a PMMA device with a carrier, fluid, and reflector layer 0.375, 0.250 and 0.375 mm thick, respectively. A standing wave is set up across the layers with a pressure node located in the fluid channel.

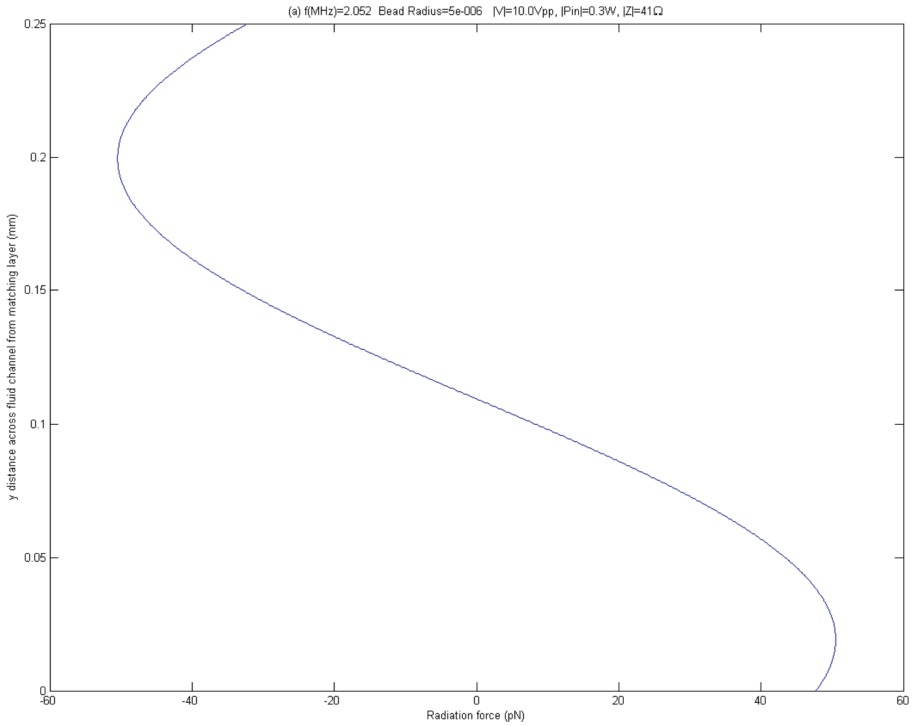


Figure 3: Corresponding force profile for Figure 2 for a 10 µm bead in the predicted acoustic pressure field. The diagram depicts the forces generated on a spherical bead in the fluid chamber. The carrier layer would be at the bottom of the diagram and the reflector at the top as is the case for the calibration described later.

thicknesses: 0.175, 0.25, and 0.375 mm. Combinations of layers were modelled in a one dimensional MATLAB model [Hill et al., 2002] and an air backing was assumed as the terminating material. The model uses an "impedance transfer" approach to relate the mechanical impedances between different layers within the device, and then uses this to derive an input electrical impedance which is driven by an electromechanical representation of the piezoceramic transducer. A device with 0.375 mm outer layers with a 0.250 mm fluid layer was identified for use in experiments. Strong acoustic forces with good node positioning and no anti-nodes in the fluid chamber were predicted; see Figure 2 and Figure 3.

Usually, glass and silicon devices are designed to fit an exact half wave in the fluid chamber; when this occurs the magnitude of forces generated are higher, but are sensitive to changes in the speed of sound in the fluid layer. In the polymer devices, the impedance differences between the PMMA and the fluid layer are small. Combined with the lower Q-factor of the polymer devices, it is less critical that an exact half wave (or multiple thereof) is set up within the fluid channel. Because of this, the design should be optimized for a resonance across the entire device. If this can be matched to that of the free transducer, a strong pressure amplitude will be set up across the device. It is then down to the ordering and thickness of the layers to position the node as required in the fluid chamber.

Marine micro sensors incorporating ultrasonic particle manipulation techniques will need to operate effectively in a variety of environments. The temperatures will vary from 45 to -2 degrees [NASA, n.d.]. This will change the speed of sound in water, which will affect the resonant frequency. The other main factor affecting the working frequency is salinity [Coates, 1990] which can vary from 0.5 parts per thousand (ppt) in fresh water to nearly 400 ppt at the Dead Sea [ONR, n.d.]. One disadvantage of designing in glass and silicon devices, when the speed of sound of the fluid is going to change, is that the variations may cause an anti-node to appear close to either the carrier/fluid or reflector/fluid boundary. This will usually be against the objectives of the device. By designing in polymers, any fraction of a wavelength can be set up across the fluid channel, meaning that changes in the speed of sound of the fluid are less likely to result in an anti-node in the device.

Another advantage of polymer devices is the positive force away from the fluid/solid boundaries towards the centre of the channel. In a more conventional half wave device, the force at the boundary is zero, meaning that particles close to the boundary experience very small forces. This means that some particles may not experience high enough forces to overcome sedimentation effects. In the polymer device, less than half a wavelength is present in the fluid channel, meaning there are forces acting on particles very close to the boundaries. In fact, the design of the device can be tailored to ensure that a large enough force is present at the carrier layer to overcome sedimentation. To maximize the forces on particles at the fluid/solid interfaces requires the design of a quarter wavelength device with a central node, meaning there is a force maximum at each fluid/solid boundary.

## DEVICE CALIBRATION

An easy and quick method for producing polymer devices for ultrasonic particle manipulation is to mill them from readily available PMMA sheets. Fluid channels were milled into one piece of PMMA and two other sheets were milled to size. The sheets were bonded together using a solvent technique involving 33% acetone with 67% ethanol [Harris et al., 2010]. The solution was placed on the surfaces to be bonded and the pieces were brought into contact. Force was applied to the sheets and after 15 minutes excess solution was syringed from the chip. The finished chips were annealed for four hours at 85°C to relieve internal stress.

To measure the acoustic pressure within the fluid chamber, voltage drop analysis experiments were undertaken. The gravitational force, $F_g$, on a 10 µm diameter spherical polystyrene bead is equal to 0.282 pN; Table 1.

| Parameter | Value |
|---|---|
| $\rho_{bead}$ | 1055 kg m$^{-3}$ |
| $\rho_{fluid}$ | 1000 kg m$^{-3}$ |
| $R$ | 5 x 10$^{-6}$ m |
| $G$ | 9.81 m s$^{-2}$ |

Table 1: Parameters used to calculate the gravitational force acting on a 10 µm bead in water.

The minimum voltage which levitates a bead must be equal to the gravitational force acting on the bead. Equation 1 shows the force generated on the bead and is greatest when sin ($2kx$) is equal to 1. The acoustic contrast factor for a polystyrene bead in water is equal to 0.15. From here the energy density can be calculated using a value of $k$ of 8700 m$^{-1}$ and is equal to 0.137 J m$^{-3}$ when the bead is just levitating. The pressure, $P_d$, will then be given by:

$$P_d = \sqrt{4\epsilon\rho_f {c_f}^2} \quad (4)$$

By recording the voltage at which a bead is just levitated, it is possible to calculate the pressure at a higher voltage, $P_1$.

$$P_1 = P_d \times \frac{V_1}{V_d} \quad (5)$$

A solution containing 10 µm diameter beads was fed into a trial device and 10 $V_{pp}$ was applied to a 4 x 30 mm wide transducer. Once a bead was captured in the acoustic forces within the device, the voltage was lowered until the forces acting on the bead were insufficient to levitate the bead, 1.6 $V_{pp}$. The acoustic pressure (P) within the chips, measured through voltage-drop analysis on a 10 µm polystyrene bead, was equal to 3.5 x 10$^4$ x Pa, at 1.6 $V_{pp}$. This corresponds to an energy density of 5.38 J m$^{-3}$ at a voltage of 10 $V_{pp}$. Impedance measurements were taken and compared with the output from the one dimensional model. The measurements showed a resonance at 2.1 MHz which matched well with the model (Figure 4).

## METHODS AND MATERIALS

The initial calibration experiments showed that the PMMA devices are capable of moving polystyrene beads away from the walls of the fluid channel. To continue the work, a set of matching PMMA devices was constructed using the sheets supplied by Cadillac Plastic

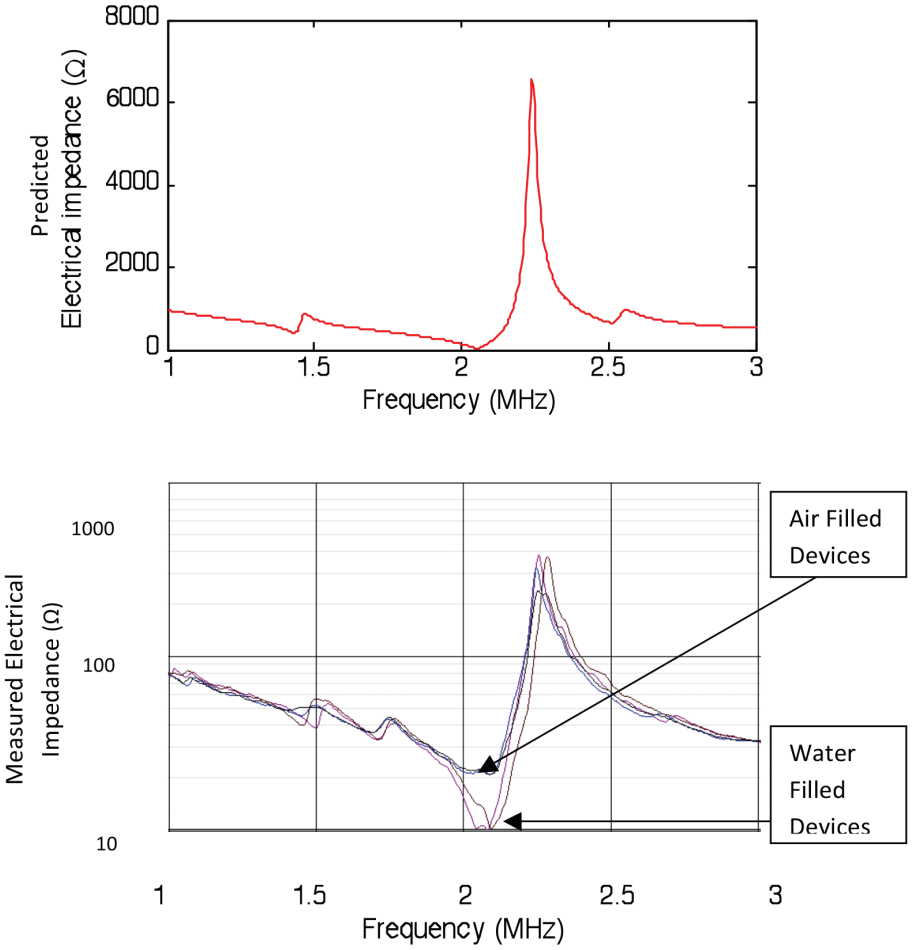


Figure 4: The predicted impedance plot is shown above and is compared with the measured impedance for two 0.375, 0.25, 0.375 mm polymer devices. The main resonance is predicted at just over 2 MHz with smaller resonances just below 1.5 MHz and at approximately 2.5 MHz. The measured plot shows a resonance at just over 2 MHz as predicted, with a smaller resonance just below 1.5 MHz. An extra resonance is seen at approximately 1.7 MHz which could be due to a resonance in a different dimension that would not be predicted using the one dimensional MATLAB model. The black and blue plots show the device with an air filled fluid chamber. The purple and brown lines show a water-filled cavity. The resonance is more pronounced and drops to a lower impedance. There is good repeatability between the two devices.

that had been cut down to standard microscope slide dimensions, 25 mm x 75 mm. The 250 µm thick slides had a fluid channel 3.8 mm wide and 50 mm long cut into the centre of each slide. The comparatively wide fluid channel gave a large surface area for biofilms to form on, and a convenient way of microscopically imaging them.

Half the 375 µm slides had holes 1 mm diameter drilled through them for fluidic access so as to line up with the ends of the fluid channel in the 250 µm slide. The 2:1 ethanol:acetone method was used to bond the slides together in a 375, 250, 375 µm sandwich. Fluid connectors were glued in place using Epotek 320. The slides were annealed at 85°C for four hours. A clamp was designed such that a 1 mm thick lead zirconate titanate (PZT) transducer could be held against the polymer slide. The PZT was milled into 4 x 30 mm pieces.

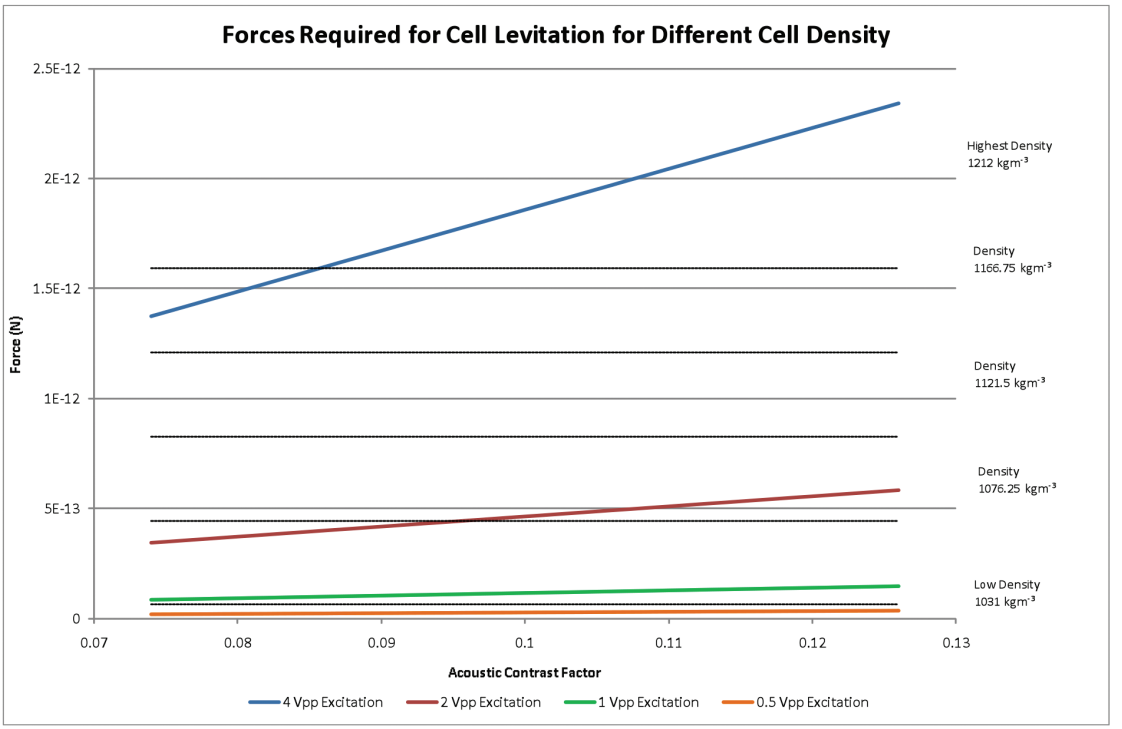


**Figure 5: The expected forces generated at different excitation voltages over the expected range in the acoustic contrast factor. The dotted lines indicate the gravitational forces that the cells would experience over the range of cell densities that the bacteria cells are likely to fall between. The coloured lines indicate the expected forces generated at different voltages. At 4 $V_{pp}$, the acoustic force should be strong enough for total cell levitation whatever the properties of the cells are. At 0.5 $V_{pp}$, the generated forces would not be enough to overcome gravitational forces even if the cells were at the lower end of the expected cell density. The values used for this graph were based on a particle with a radius of 0.59 µm which is the smallest equivalent sphere cell size expected in the *V. natriegens*.**

The expected forces were plotted along with the gravitational forces for a range of cell densities and ultrasonic excitation voltages (Figure 5). At the highest excitation voltage, the forces generated were expected to be strong enough for total cell levitation. At the lower voltages, the forces generated would not be expected to be sufficient for total cell levitation, but would limit bacteria adhesion. In these experiments, the acoustic forces were used to manipulate cells within a vertically flowing fluid channel. As a result, the force generated did not need to overcome gravitational forces and so a lower excitation voltage should be sufficient to manipulate the cells.

Bottles of 3MN solution were prepared and autoclaved along with steel connectors and polypropylene tubing for the peristaltic pump. Each 1 litre bottle had four polymer slides connected via a peristaltic pump to form a closed system. The polymer slides were sterilized using ethanol for 15 minutes before being air dried. Three experiments ran in series, each with two ultrasonically activated slides and two control slides. The maximum voltage used was 4 $V_{pp}$ at which magnitude the acoustic force should be strong enough for total cell levitation. Details of the experiment are summarized in Table 2.

For consistency between experiments, each batch of seawater was conditioned on a heated stirring plate at 25°C at 60 rpm. At the beginning of each experiment, the 3MN solution was seeded with *V. natriegens*. Each

| Experiment | Slide Number | Excitation Voltage $V_{pp}$ |
|---|---|---|
| 1 | 1 | 4 |
| 1 | 2 | 2 |
| 1 | 3 | 0 |
| 1 | 4 | 0 |
| 2 | 5 | 1 |
| 2 | 6 | 2 |
| 2 | 7 | 0 |
| 2 | 8 | 0 |
| 3 | 9 | 1 |
| 3 | 10 | 0.5 |
| 3 | 11 | 0 |
| 3 | 12 | 0 |

Table 2: Summary of the experiments undertaken with the polymer slides.

experiment ran for one week, when the slides were flushed with milliQ water. Each slide was then treated with 5-Cyano-2,3-ditolyl tetrazolium chloride (CTC) dye for actively respiring cells and 4',6-diamidino-2-phenylindole (DAPI) dye for the total number of cells [Rodriguez et al., 1992; Cappelier et al., 1997; Sieracki et al., 1999; Pyle et al., 1995].

Images were taken using an inverted fluorescence microscope (Olympus IX71) along the length of the internal surfaces parallel to the PZT transducer. Three series of images were taken along each surface, one at each edge and one along the centre of the channel, all at a magnification of 10×. A diagram of the imaging method is shown in Figure 6. Images were taken using fluorescence microscopy using the appropriate filters for each of the dyes used. Cellprofiler software was used to analyze and calibrate the images [Carpenter et al., 2006].

## IMAGE ANALYSIS

The first 200 pixels were discarded from the outer edge of each image reducing edge effect variation from lighting and focus, evanescent illumination, and avoiding any overlapping of sections of the fluid channel. The second filter applied to the images was used to enhance individual bacteria against the background image and to remove large contaminants from the image. Objects consisting of 10 or more pixels were removed. Objects of 10 or less pixels were sharpened relative to the background. Filtering for larger objects had no effect on the final quantity of bacteria identified, but increased dramatically the computational time required. Dropping object detection below 10 pixels reduced dramatically the number of bacteria identified and visual inspection confirmed that bacteria were not being counted; see Figure 7. An example image is shown in the pre and post enhanced and supressed stage (Figure 8).

The next filter applied to the images was used to count the number of bacteria cells in each image. The module was set to identify objects between 2 and 10 pixels across using intensity peaks.


Figure 6: A diagram describing the method used to image the surfaces of the polymer slides. Images were taken along the length of each fluid channel following the three paths set out above as "Edge 1, Middle, and Edge 2." Images were taken from left to right moving along the channel.

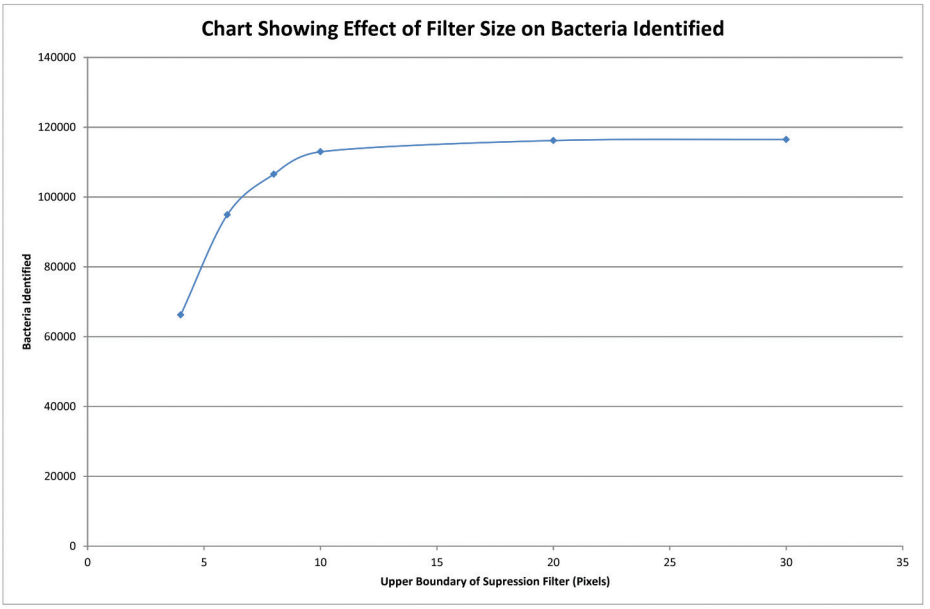


Figure 7: Chart showing the effects of the upper limit of the suppression filter on the total number of bacteria identified. Down to approximately 10 pixels, there is negligible change. Above this, computational time increases dramatically. Below this, bacteria are being removed from the image and therefore not counted. A sample of 87 DAPI images was used to produce this graph.

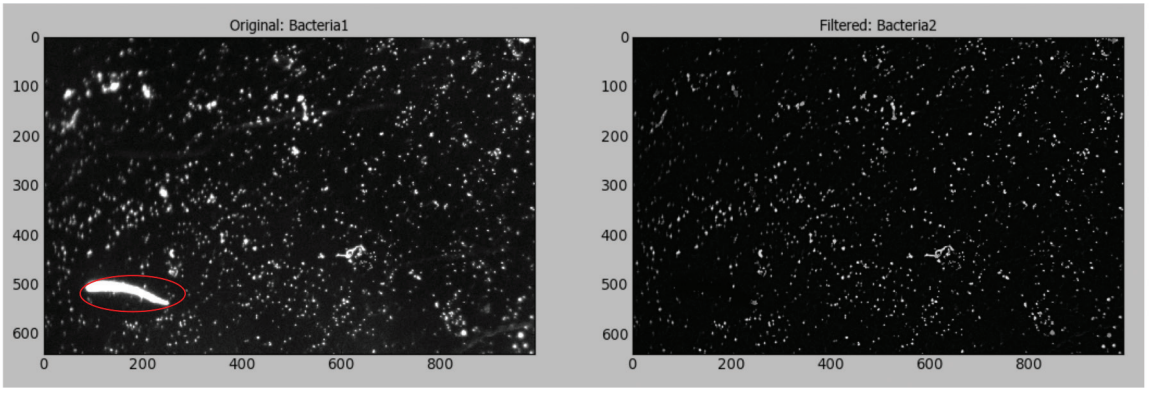


Figure 8: Example image showing the original image on the left, including a contaminant circled in red. After applying the suppression filter, the contaminant is removed from the image and individual bacteria have been enhanced relative to the background.

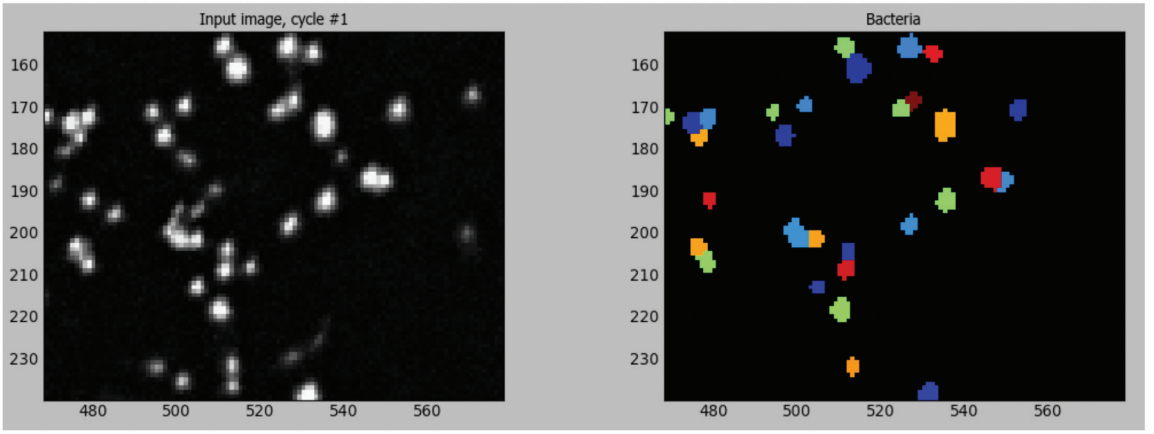


Figure 9: Close up image of a series of bacteria cells that have been undercounted due to the minimum threshold for bacteria being too high at 3 pixels. The left image shows the original and the right image shows what has been identified as bacteria; each coloured dot represents a bacteria cell being counted. There are bacteria visible to the eye in the left image that have not been counted as a bacteria in the right image as they are too small. Changing the threshold to 2 pixels alleviated this problem.

Using a minimum object size of 1 resulted in exceptionally high numbers of objects counted as bacteria being identified within the image. Visual analysis confirmed that variations in background intensity were being recorded as bacteria incorrectly. Increasing the minimum bacteria size to 3 pixels caused a drop in the number of bacteria being identified and visual inspection shows that it fails to identify bacteria that are present (Figure 9).

The upper bound for identifying objects was significantly less critical down to 10 pixels. Below this, large bacteria are not counted and thus the count was underestimated. In total, 3,532 images were analyzed for statistical rigor and the same settings were used for the DAPI images as the CTC images.

Applying these methods to the images had a strong positive effect on the correlation between the image intensity and number of bacteria counted. This can be seen in Figure 10 and Figure 11.

The aim of the experiment was to reduce biofilm formation in polymer microfluidic channels and show the effects in a quantitative way. The following section will show the effects of ultrasonic excitation on biofilm formation, cell metabolism, and positioning.

## RESULTS

The ultrasonic excitation reduced the total quantity of bacteria adhered to the surface of the polymer slides; see Figure 12. Interestingly, the quantity of bacteria identified in the control slides varied noticeably between experiments but the variation between control slides in the same experiment was within one standard error of the other control slide in that experiment. Each individual experiment showed a reduction in the total quantity of bacteria adhered to the surface of the polymer slide when ultrasonic excitation was used.

Despite the variations in the quantity of bacteria in the control slides between experiments, a

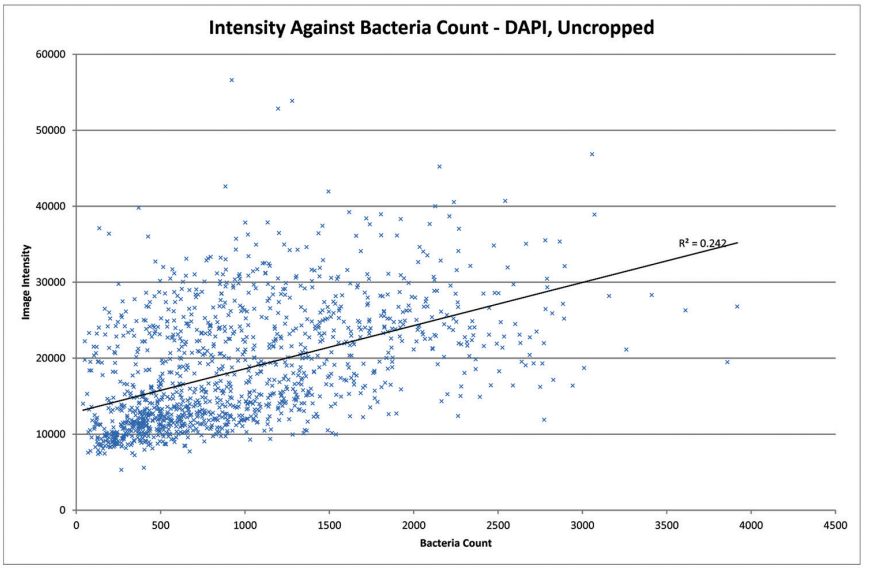


Figure 10: A plot of image intensity against bacteria counted for the original uncropped images. The $R^2$ value is low at 0.242 implying poor correlation.

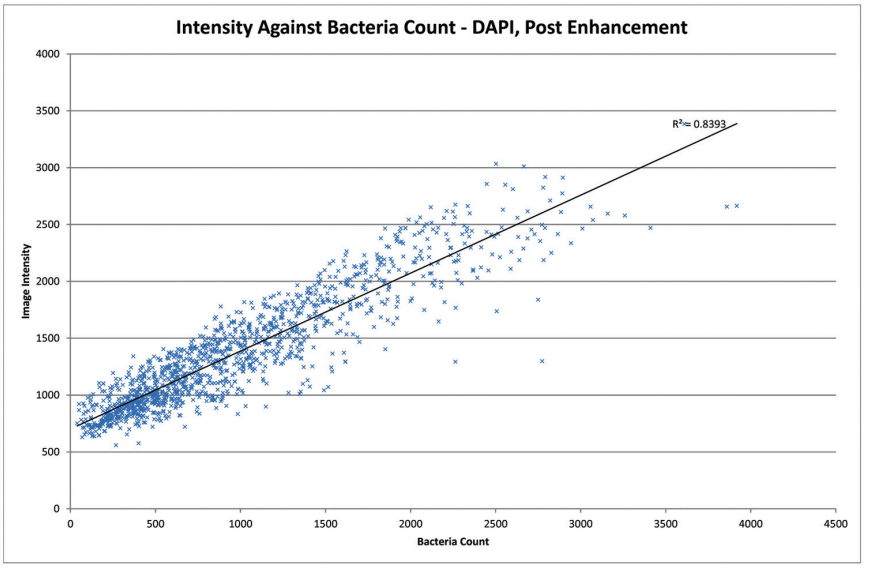


Figure 11: A plot showing strong correlation between image intensity and the number of bacteria identified. An improved $R^2$ value of 0.8393 was achieved.

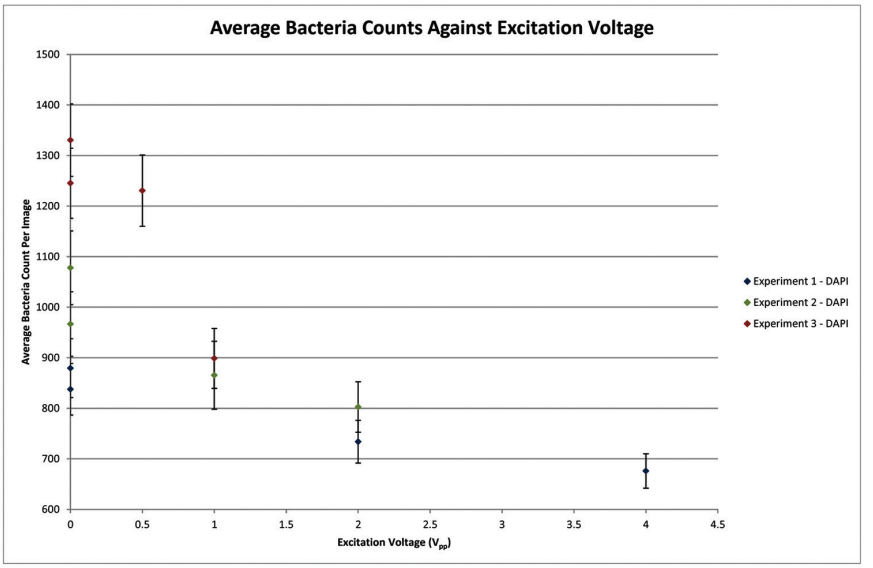


Figure 12: Excitation voltage is plotted on the abscissa and the ordinate refers to the average number of DAPI stained bacteria identified in each image. Error bars are defined as ± the standard error. Readings from the same experiment share colour. DAPI readings indicate total cell count. Every experiment showed a reduction in total biofilm formation from ultrasonic excitation.

reduction in the total quantity of bacteria in the slides was observed by the addition of ultrasonic standing wave techniques.

A similar but less pronounced drop in bacteria numbers was seen in the actively respiring bacteria; see Figure 13. Experiment 1 showed a significant drop in the quantity of actively respiring bacteria in the ultrasonically active slides. Experiment 2 showed a marginal drop in actively respiring bacteria. Experiment 3 showed contradicting results for the slides when powered at 0.5 $V_{pp}$ and 1 $V_{pp}$. The lower powered slide led to a significant increase in the number of actively respiring cells, while the higher powered slide led to a significant drop. Variation between control slides of the same experiment is greater than in the total cell count. This can also be seen by the significant differences between slides with the same ultrasonic excitation but in different experiments. While in the total cell count they were similar, in the actively respiring bacteria they are vastly different.

Ultrasonic excitation in a polymer microfluidic channel can lead to a reduction in the quantity of bacteria adhering to a surface. Even at particularly low voltages, a reduction in biofilm formation was seen. While the forces generated at 0.5 $V_{pp}$ would not be sufficient to levitate cells even if they had favourable properties (density, acoustic contrast factor), the slides were oriented vertically. This means that the forces only need to overcome any attractive forces between the cells and the surface of the slide.

It is important to understand any effects that ultrasonic excitation has on the behaviour of bacteria cells. By plotting total bacteria counts and actively respiring bacteria counts, it can be seen there is no real variation in how a colony of cells behave with and without ultrasonic excitation (Figure 14). Experiments 1 and 2 show a decrease in the total number of bacteria and the number of actively respiring bacteria. This is consistent with the idea that ultrasonic excitation only affects the quantity of bacteria that adheres to a surface and does not affect the growth or death of the bacteria once it has adhered. Experiment 3 follows this trend excluding the slide that was powered at 0.5 $V_{pp}$; this slide shows a significant increase in the ratio of respiring bacteria to non-active bacteria. When plotted as a percentage, it is clear that ultrasonic excitation does not have a noticeable effect on the ratio of active to total cells. A slight reduction in the proportion of actively respiring cells can be seen excluding the slide powered at 0.5 $V_{pp}$ which shows a significant increase in actively respiring bacteria; see Figure 15.

The presence of ultrasonic excitation not only reduces the adherence of bacteria to a surface, but also appears to inhibit cell respiration. In every experiment, the chip with the highest level of ultrasonic excitation had the lowest percentage of respiring cells. The total cell density is vastly different in every experiment; it can be expected that this would lead to variations in the percentage of actively respiring cells, as competition for nutrients and concentrations of waste metabolites differs. This could explain why there is significant variation in the percentage of metabolizing cells between slides that were powered at the same excitation voltage but in different experiments.

The obvious exception to this is the slide powered at 0.5 $V_{pp}$ in experiment 3. The quantity

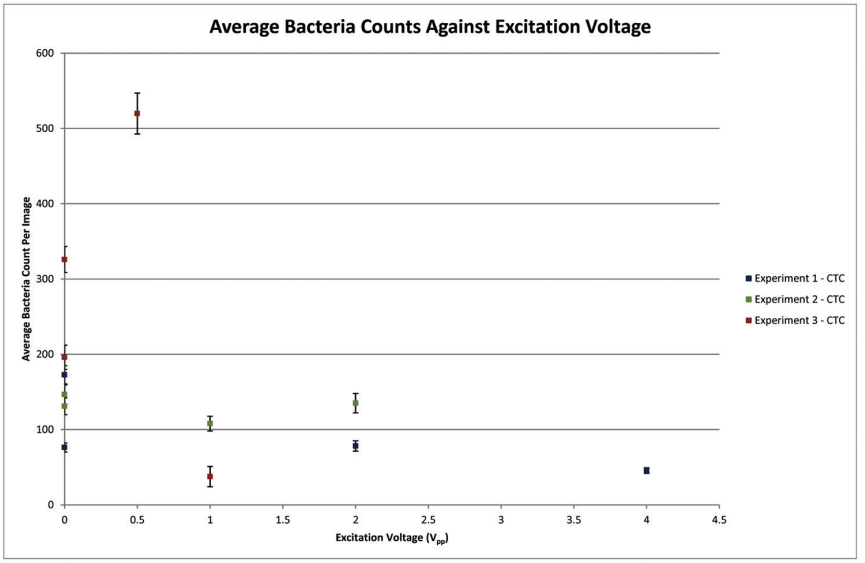


Figure 13: Excitation voltage is plotted on the abscissa and the ordinate refers to the average number of CTC stained bacteria identified in each chip. Error bars are defined as ± the standard error. Readings from the same experiment share colour. CTC readings indicate actively respiring cells.

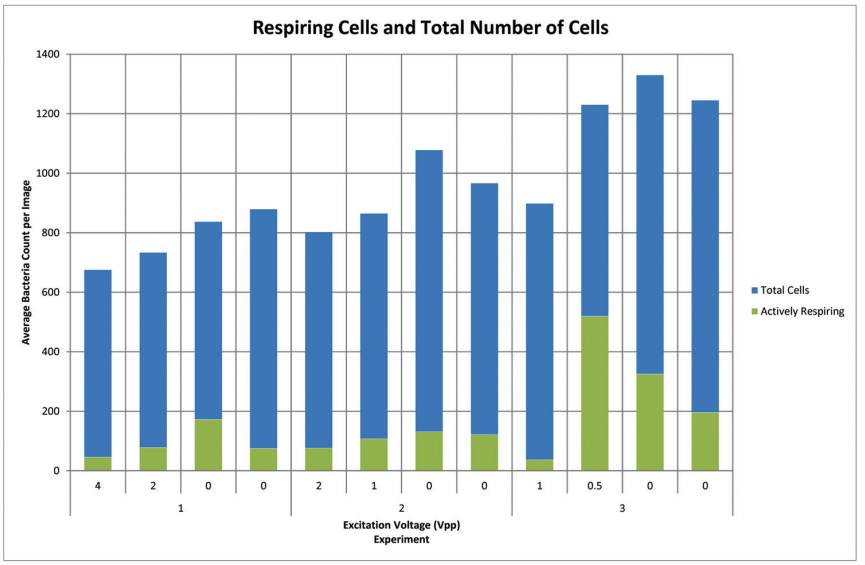


Figure 14: A graph showing the effects of ultrasonic excitation on the ratio of actively respiring cells to total cells. Each experiment is grouped together and shown in descending order of ultrasonic excitation. There is no noticeable difference in the ratio of actively respiring to non-active cells excluding the slide powered at 0.5 $V_{pp}$.

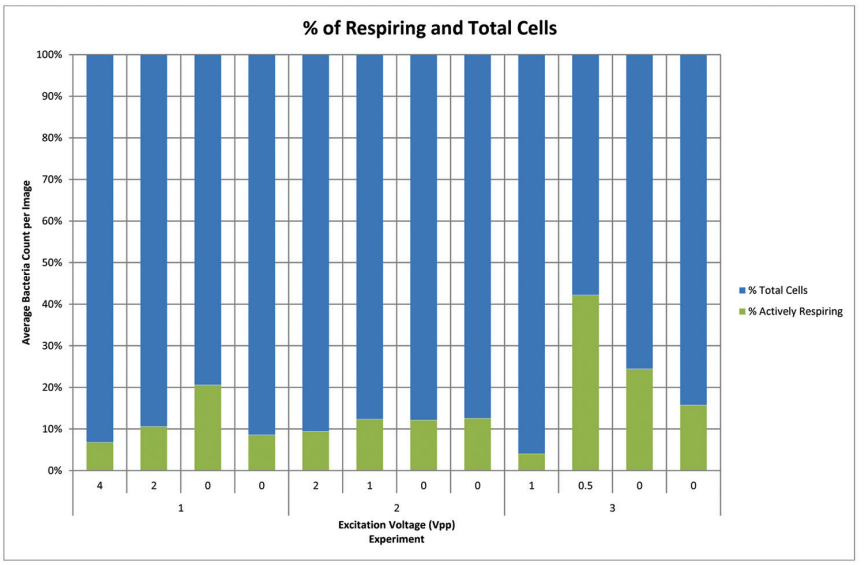


Figure 15: When the data is plotted as a percentage, it shows that ultrasonic excitation does not have a noticeable impact on the proportion of cells actively respiring and the total number of cells. If anything, a slight decrease in percentage of actively respiring cells can be seen.

of bacteria that is actively respiring is significantly higher than in any other slide. One potential reason for this could be that at such low levels of ultrasonic excitation, variations within the cell population in terms of size, density, and acoustic contrast factor could cause a bias in the bacteria that attach to the surface. For instance, the forces acting on the bacteria that have a low acoustic contrast factor will be less than the forces on bacteria with a high acoustic contrast factor. If the bacteria that are less likely to respire have a high acoustic contrast factor, then this would lead to a percentage increase in respiring bacteria on the surface of the slide but an overall reduction in bacteria numbers. As the excitation voltage increases, the acoustic forces would be sufficient to act on all the bacteria cells and the percentage discrepancy would stop.

While no firm conclusions can be drawn about the effect of ultrasonic excitation on the metabolism of bacteria cells, if true it would be an additional benefit. The metabolites produced by bacteria will have a negative impact on the accuracy of readings taken within a microfluidic oceanographic sensor; therefore, reducing the quantity of metabolizing cells will lead to more accurate and repeatable readings.

One potential mechanism for the reduction in the percentage of metabolizing cells could be that cells adhere to the surface but still experience the acoustic radiation force. This could be exerting a stress on the cell which reduces the ability of the cell to metabolize. The idea fits with the fact that in each experiment the slide with the highest level of ultrasonic excitation had the lower percentage of metabolizing bacteria.

## CONCLUSIONS

Biofouling is one of the main constraints on the working life of oceanographic sensors for two main reasons:

- The physical presence of the film will reduce fluid flow and could potentially cover sensing surfaces.
- The biological presence of the film will affect the readings taken through the uptake and release of chemicals.

This work has presented a novel and low power method to reduce the formation of biofilms in polymer microfluidic channels. Before this work, attempts to use ultrasonic techniques to reduce biofouling relied on high power acoustic streaming used over short timescales to actively lift adhered bacteria.

The power requirements of these polymer devices was low at less than 1 W. Throughout these experiments, twelve devices were created that showed very similar acoustic properties and the same ultrasonic frequency was used for all the experiments. To manufacture twelve comparable devices in silicon or glass would be difficult to achieve, as minor variations in dimensions cause large differences in the frequency response.

This series of experiments used a thorough image analysis technique to show a reduction in the total number of bacteria and in the actively respiring bacteria. The results showed a general decline as the voltage applied increased which is consistent with theory. The percentage of actively respiring bacteria appeared to reduce as the strength of the acoustic field increased. It

was not possible to confirm if this was due to the acoustic forces or natural variations. The methods and analysis used throughout these experiments was robust, detailed and provided significant quantitative evidence that ultrasonic particle manipulation techniques can reduce the formation of biofilms over the relatively long period of time of a week.

ACKNOWLEDGMENT

Michael Gedge was funded by Engineering and Physical Sciences Research Council grant EP/E016774/1, *Ruggedised MicroSystem Technology for Marine Measurement*. The authors acknowledge valuable input from Professor Hywel Morgan and Dr. Matt Mowlem in the initial stages of the work, and from Drs. Dyan Ankrett and Peter Glynne-Jones in the implementation of the experiments.

REFERENCES

Antfolk, M.; Muller, P.B.; Augustsson, P.; Bruus, H.; and Laurell, T. [2014]. *Focusing of sub-micrometer particles and bacteria enabled by two-dimensional acoustophoresis*. Lab on a Chip, Vol. 14, No. 15, pp. 2791-2799. doi:10.1039/C4LC00202D.

Augustsson, P.; Persson, J.; Ekstrom, S.; Ohlin, M.; and Laurell, T. [2009]. *Decomplexing biofluids using microchip based acoustophoresis*. Lab on a Chip, Vol. 9, No. 6, pp. 810-818. doi:10.1039/b811027a.

Bott, T.R. [2000]. *Biofouling control with ultrasound*. Heat Transfer Engineering, Vol. 21, No. 3, pp. 43-49. doi:10.1080/014576300270898.

Bruus, H. [2012A]. *Acoustofluidics 7: The acoustic radiation force on small particles*. Lab on a Chip, Vol. 12, No. 6, pp. 1014-1021. doi:10.1039/C2LC21068A.

Bruus, H. [2012B]. *Acoustofluidics 10: scaling laws in acoustophoresis*. Lab on a Chip, Vol. 12, No. 9, pp. 1578-1586. doi:10.1039/C2LC21261G.

Cappelier, J.M.; Lazaro, B.; Rossero, A.; Fernandez-Astorga, A.; and Federighi, M. [1997]. *Double staining (CTC-DAPI) for detection and enumeration of viable but non-culturable* Campylobacter jejuni *cells*. Veterinary Research, Vol. 28, No. 6, pp. 547-555.

Carpenter, A.E.; Jones, T.R.; Lamprecht, M.R.; Clarke, C.; Kang, I.H.; Friman, O.; Guertin, D.A.; Chang, J.H.; Lindquist, R.A.; Moffat, J.; Golland, P.; and Sabatinia, D.M. [2006]. *CellProfiler: image analysis software for identifying and quantifying cell phenotypes*. Genome Biology, Vol. 7, No. 10, pp. R100. doi:10.1186/gb-2006-7-10-r100.

Carugo, D.; Octon, T.; Messaoudi, W.; Fisher, A.L.; Carboni, M.; Harris, N.R.; Hill, M.; and Glynne-Jones, P. [2014]. *A thin-reflector microfluidic resonator for continuous-flow concentration of microorganisms: a new approach to water quality analysis using acoustofluidics*. Lab on a Chip, Vol. 14, No. 19, pp. 3830-3842. doi:10.1039/C4LC00577E.

Cheng, S.; Lau, K-T.; Chen, S.; Chang, X.; Liu, T.; and Yin, Y. [2010]. *Microscopical observation of the marine bacterium* Vibrio Natriegeus *growth on metallic corrosion*. Materials and Manufacturing Processes, Vol. 25, No. 5, pp. 293-297 doi:10.1080/10426911003747642.

Chien, A.C.; Hill, N.S.; and Levin, P.A. [2012]. *Cell size control in bacteria*. Current Biology, Vol. 22, No. 9, pp. R340-R349.

doi:10.1016/j.cub.2012.02.032.

Coates, R.F.W. [1990]. *Underwater Acoustic Systems* (Macmillan new electronics series). London: Palgrave Macmillan.

Delauney, L.; Compère, C; and Lehaitre, M. [2010]. *Biofouling protection for marine environmental sensors*. Ocean Science, Vol. 6, pp. 503-511. doi:10.5194/os-6-503-2010.

Denkin, S.M. and Nelson, D.R. [1999]. *Induction of protease activity in* Vibrio anguillarum *by gastrointestinal mucus*. Applied and Environmental Microbiology, Vol. 65, No. 8, pp. 3555-3560.

Eagon, R.G. [1962]. Pseudomonas Natriegens, *a marine bacterium with a generation time of less than 10 minutes*. Journal of Bacteriology, Vol. 83, No. 4, pp. 736-737.

Fagerbakke, K.M.; Heldal, M.; and Norland, S. [1996]. *Content of carbon, nitrogen, oxygen, sulfur and phosphorus in native aquatic and cultured bacteria*. Aquatic Microbial Ecology, Vol. 10, No. 1, pp. 15-27.

Field, C.B.; Behrenfeld, M.J.; Randerson, J.T.; and Falkowski, P. [1998]. *Primary production of the biosphere: integrating terrestrial and oceanic components*. Science, Vol. 281, No. 5374, pp. 237-240.

Fitts, C.R. [2013]. *Physical properties* (pp. 23-45). In Groundwater Science (Second Edition). Boston: Academic Press: Boston.

Gor'Kov, L.P. [1962]. *On the forces acting on a small particle in an acoustic field in an ideal fluid*. Soviet Physics, Vol. 6, No. 9, pp. 773-775.

Hall-Stoodley, L.; Costerton J.W.; and Stoodley, P. [2004]. *Bacterial biofilms: from the natural environment to infectious diseases*. Nature Reviews Microbiology, Vol. 2, No. 2, pp. 95-108. doi:10.1038/nrmicro821.

Harris, N.; Keating, A.; and Hill, M. [2010]. *A lateral mode flow-through PMMA ultrasonic separator*. Conference proceedings, Asia-Pacific Conference of Transducers and Micro-Nano Technology, Perth, Western Australia.

Hill, M.; Shen, Y.; and Hawkes, J.J. [2002]. *Modelling of layered resonators for ultrasonic separation*. Ultrasonics, Vol. 40, Nos. 1-8, pp. 385-392. doi:10.1016/S0041-624X(02)00127-0.

Hultstrom, J.; Manneberg, O.; Dopf, K.; Hertz, H.M.; Brismar, H.; and Wiklund, M. [2007]. *Proliferation and viability of adherent cells manipulated by standing-wave ultrasound in a microfluidic chip*. Ultrasound in Medicine and Biology, Vol. 33, No. 1, pp. 145-151.

King, L.V. [1934]. *On the acoustic radiation pressure on spheres*. Proceedings of the Royal Society of London. Series A, Mathematical and Physical Sciences, Vol. 147, No. 861, pp. 212-240. doi:10.1098/rspa.1934.0215.

Kundt, L. and Lehman, O. [1874]. *Longitudinal vibrations and acoustic figures in cylindrical columns of liquid*. Annal Physik, Vol. 153.

Lehaitre, M.; Delauney, L.; and Compère, C. [2008]. *Biofouling and underwater measurements*. In Babin, M.; Roesler, C.S.; and Cullen, J.J. (Eds.), Real-time coastal observing systems for marine ecosystem dynamics and harmful algal blooms, pp. 463-493. France: UNESCO Publishing.

Lei, J.; Hill, M.; and Glynne-Jones, P. [2014]. *Numerical simulation of 3D boundary-driven acoustic streaming in microfluidic devices*. Lab on a Chip, Vol. 14, No. 3, pp. 532-41. doi:10.1039/c3lc50985k.

Mårdén, P.; Tunlid, A.; Malmcrona-Friberg, K.; Odham, G.; and Kjelleberg, S. [1985]. *Physiological and morphological changes during short term starvation of marine*

*bacterial islates*. Archives of Microbiology, Vol. 142, No. 4, pp. 326-332.

Mott, I.E.C.; Stickler, D.J.; Coakley, W.T.; and Bott, T.R. [1998]. *The removal of bacterial biofilm from water-filled tubes using axially propagated ultrasound*. Journal of Applied Microbiology, Vol. 84, No. 4, pp. 509-514. doi:10.1046/j.1365-2672.1998.00373.x.

NASA Earth Observatory [n.d.]. *Global maps, sea surface temperature*. Retrieved from http://earthobservatory.nasa.gov/GlobalMaps/view.php?d1=MYD28M.

ONR Office of Naval Research [n.d.] *Ocean water: salinity*. Retrieved from http://www.onr.navy.mil/Focus/ocean/water/salinity1.htm.

Pyle, B.H.; Broadaway, S.C.; and McFeters, G.A. [1995]. *Factors affecting the determination of respiratory activity on the basis of cyanoditolyl tetrazolium chloride reduction with membrane filtration*. Applied and Environmental Microbiology, Vol. 61, No. 12, pp. 4304-4309.

Rodriguez, G.G.; Phipps, D.; Ishiguro, K.; and Ridgway, H.F. [1992]. *Use of a fluorescent redox probe for direct visualization of actively respiring bacteria*. Applied and Environmental Microbiology, Vol. 58, No. 6, pp. 1801-1808.

Sadhal, S.S. [2012]. *Acoustofluidics 13: analysis of acoustic streaming by perturbation methods*. Lab on a Chip, Vol. 12, No. 13, pp. 2292-2300. doi:10.1039/c2lc40202e.

Salta, M.; Wharton, J.A.; Blache, Y.; Stokes, K.R.; and Briand, J-F. [2013]. *Marine biofilms on artificial surfaces: structure and dynamics*. Environmental Microbiology, Vol. 15, No. 11, pp. 2879-2893. doi:10.1111/1462-2920.12186.

Sankaranarayanan, S.K.R.S.; Cular, S.; Bhethanbotla, V.R.; and Joseph, B. [2008]. *Flow induced by acoustic streaming on surface acoustic wave devices and its application in biofouling removal: a computational study and comparisons to experiment*. The American Physical Review, Vol. 77, No. 6. doi:http://dx.doi.org/10.1103/PhysRevE.77.066308.

Sieracki, M.E.; Cucci, T.L.; and Nicinski, J. [1999]. *Flow cytometric analysis of 5-cyano-2,3-ditolyl tetrazolium chloride activity of marine bacterioplankton in dilution cultures*. Applied and Environmental Microbiology, Vol. 65, No. 6, pp. 2409-2417.

Sharma, R.V.; Edwards, R.T.; and Beckett, R. [1998]. *Analysis of bacteria in aquatic environments using sedimentation field-flow fractionation: (II) physical characterization of cells*. Water Research, Vol. 32, No. 5, pp. 1508-1514. doi:10.1016/S0043-1354(97)00398-9.

Srivastava, S and Srivastava, P.S. [2003]. *Understanding bacteria*. Dordrecht and Norwell: Kluwer Academic Publishers.

Toubal, M.; Asmani, M.; Radziszewski, E.; and Nongaillard, B. [1999]. *Acoustic measurement of compressibility and thermal expansion coefficient of erythrocytes*. Physics in Medicine and Biology, Vol. 44, No. 5, pp. 1277-1287. doi:10.1088/0031-9155/44/5/313.

Townsend, R.J.; Hill, M.; Harris, N.R.; and White, N.M. [2004]. *Modelling of particle paths passing through an ultrasonic standing wave*. Ultrasonics, Vol. 42, Nos. 1-9, pp. 319-324.

Wang, T.C. and Lee, C.P. [1998]. *Radiation pressure and acoustic levitation*. In Hamilton, M.F. and Blackstock, D.T. (Eds.), Nonlinear acoustics. New York: Academic Press.

Whelan, A. and Regan, F. [2006]. *Antifouling strategies for marine and riverine sensors*.

Journal of Environmental Monitoring, Vol. 8, No. 9, pp. 880-886. doi:10.1039/B603289C.

Wiklund, M. [2012]. *Acoustofluidics 12: biocompatibility and cell viability in microfluidic acoustic resonators*. Lab on a Chip, Vol. 12, No. 11, pp. 2018-2028. doi:10.1039/c2lc40201g.

WOR World Ocean Review [2010]. *Marine fisheries – the state of affairs*. Retrieved from http://worldoceanreview.com/en/fisheries/state-of-affairs.

Yosioka, K. and Kawasima, Y. [1955]. *Acoustic radiation pressure on a compressible sphere*. Acustica, Vol. 5, No. 3, pp. 167-173.